

INTERNATIONAL SOCIETY FOR SOIL MECHANICS AND GEOTECHNICAL ENGINEERING



This paper was downloaded from the Online Library of the International Society for Soil Mechanics and Geotechnical Engineering (ISSMGE). The library is available here:

<https://www.issmge.org/publications/online-library>

This is an open-access database that archives thousands of papers published under the Auspices of the ISSMGE and maintained by the Innovation and Development Committee of ISSMGE.

The paper was published in the proceedings of the 20th International Conference on Soil Mechanics and Geotechnical Engineering and was edited by Mizanur Rahman and Mark Jaksa. The conference was held from May 1st to May 5th 2022 in Sydney, Australia.

The effect of rainfall pattern on unsaturated tropical slopes

L'effet des précipitations sur les pentes tropicales non saturées

Aizat Mohd Taib, Norinah Abd Rahman, Irfan Haziq Razali & Nur Izzi Md Yusoff

Faculty of Engineering and Built Environment, Universiti Kebangsaan Malaysia, Malaysia, amohdtaib@ukm.edu.my

Dayang Zulaika Abang Hasbollah

Faculty of Civil Engineering, Universiti Teknologi Malaysia, Malaysia

Mariati Taib

School of Housing Building and Planning, Universiti Sains Malaysia, Malaysia.

ABSTRACT: Landslides of partially saturated slopes are recurrent events especially for countries that receive abundant rainfall. Due to the wet season, heavy rainfall and thunderstorms affect the slope stability in both rural and urban areas thus disrupt the economy, social and public safety. This paper presents a parametric study of a typical rainfall in Bukit Timah, Singapore on unsaturated slope stability. The intensity of a typical rainfall is varied into several patterns to evaluate the effect on the initial pore-water pressure. The hydrological and soil properties are assigned based on the calibration of soil-water characteristic curve (SWCC) and permeability functions. The results of generated pore-water pressure profile are compared with previous numerical studies. It is found that at the crest of the slope, larger changes of negative pore-water pressure occurs compared to the toe. In addition, shallower depths of 0.64 m proved that larger negative pore-water pressure changes and faster increment of saturation due to the infiltration of rainfall. Unlike deeper soils (i.e. 1.31, 2.06 and 2.08 m), smaller changes in negative pore-water pressure are observed. Moreover, the slope height and angle and soil permeability are found to influence the rainfall infiltration too. This study, therefore, demonstrates the effect of rainfall patterns on partially saturated tropical slopes particularly the groundwater flow.

RÉSUMÉ : Les glissements de terrain de pentes partiellement saturées sont des événements récurrents surtout pour les pays qui reçoivent des précipitations abondantes. En raison de la saison des pluies, les fortes précipitations et les orages affectent la stabilité des pentes dans les zones rurales et urbaines, perturbant ainsi l'économie, la sécurité sociale et publique. Cet article présente une étude paramétrique d'une pluviométrie typique à Bukit Timah, Singapour sur la stabilité des pentes non saturées. L'intensité d'une pluie typique varie en plusieurs modèles pour évaluer l'effet sur la pression initiale de l'eau interstitielle. Les propriétés hydrologiques et du sol sont attribuées sur la base de l'étalonnage de la courbe caractéristique sol-eau (SWCC) et des fonctions de perméabilité. Les résultats du profil de pression interstitielle générée sont comparés aux études numériques précédentes. On constate qu'à la crête de la pente, des changements plus importants de la pression interstitielle négative se produisent par rapport au pied. De plus, des profondeurs plus faibles de 0,64 m ont prouvé que la pression interstitielle négative plus importante change et une augmentation plus rapide de la saturation due à l'infiltration des précipitations. Contrairement aux sols plus profonds (c'est-à-dire 1,31, 2,06 et 2,08 m), de plus petits changements de pression interstitielle négative sont observés. De plus, la hauteur et l'angle de la pente et la perméabilité du sol influent également sur l'infiltration des précipitations. Cette étude démontre donc l'effet du régime des précipitations sur les pentes tropicales partiellement saturées, en particulier l'écoulement des eaux souterraines.

KEYWORDS: Rainfall, unsaturated, tropical slopes, pore-water pressure

1 INTRODUCTION

Rainfall is well-known as the primary and triggering factor for landslides in Singapore (Toll 2001). Due to these natural disasters, losses of life and economic disruption are seen (Tsaparas et al. 2002) which also leads to many studies and investigations on partially saturated slope behaviour. Much research is undertaken particularly in the field and laboratory works, however, many studies are also conducted numerically (Mukhlisin et al. 2011, Cai & Ugai 2004 and Gasmol et al. 2000) in regards to financial and time constraints. In tropical countries with abundant rainfall especially during the wet season, it is significant to understand how prolonged and heavy rainfall can affect slope stability. Several factors are considered in the studies by analysing the historical and current rainfall features, varying wind speed, humidity and temperatures and the basic mechanical and hydrological properties of the soils. In addition, by incorporating partially saturated soils, it is interesting to acknowledge a wider perspective of the degree of saturation in soils. With the understanding that tropical soils are normally found in unsaturated conditions, the typical effects of rainfall on

slope stability shall not be applied stereotypically and directly to all slope stability cases.

To model the infiltration of rainfall and corresponding soil behaviour, the interaction of soil and water has to be carefully determined. In unsaturated soil mechanics, the soil hydraulic properties can be measured as the volumetric water content and the coefficient of permeability with respect to matric suction, by using the soil-water characteristic curve (SWCC) and permeability function respectively. The SWCC is a relationship between the water content and suction in soil while the permeability function is the relationship between the coefficient of permeability and soil suction (Zhang et al. 2004). Many equations of SWCC and permeability functions have been introduced over the decades and the popularly utilised ones are the equations by Van Genuchten (1980) and Fredlund et al. (1994).

This paper aims to model the unsaturated groundwater flow in tropical slopes with the effects of different rainfall patterns by using the SWCC and permeability function by Fredlund et al. (1994i) and Fredlund et al. (1994ii) respectively. The soil hydraulic properties are calibrated from the field data and other

soil properties are gathered from the literature. Extensive parametric studies are conducted under the influence of various rainfall intensities which are assigned in different patterns. The generated pore-water pressure is presented according to the existing and assigned rainfall patterns.

2 RAINFALL PATTERN

The investigation of unsaturated groundwater flow with the effects of different rainfall patterns contributes highly to literature. The studies of rainfall patterns, in particular, the tropical climate has been extensively undertaken. Several researchers such as Che Ghani et al. (2019), Mohd Taib (2018), Ibrahim et al. (2018), Kristo et al. (2017), Li et al. (2017), Sagitaningrum et al. (2017), El-Shafie et al. (2011), Rahimi et al. (2010), Taha et al. (2000) applied a variety of customised rainfall pattern to observe the change of behaviour in unsaturated slopes. Moreover, Ng et al. (2001) have applied advanced, central and delayed patterns on slope analysis, whereas Rahimi et al. (2010) multiplied the idealised rainfall percentage for each rainfall interval, so as to develop three recognised patterns. In their work, central rainfall has a normal distribution, unlike the advanced pattern, which shows positive and negative skews for delayed rainfall. A number of recent findings have proved that the patterns of rainfall demonstrate a significant effect on pore-water pressure generated in soils (Ng et al. 2001). It has also been highlighted that antecedent rainfall is a common cause of landslides (Ng & Shi 1998, Rahardjo et al. 2001).

2.1 Surface infiltration

The infiltration of rainfall into the slopes is influenced by many factors such as the rainfall intensities and duration, slope angle and soil hydraulic properties. These factors caused a change in infiltration rates. Much research has been undertaken to investigate all the variables. The studies include the investigations and understanding of the infiltration effects on partially saturated (McDougall & Pyrah 1998, Zhan & Ng 2004, Zhan et al. 2007, Gofar et al. 2008, Garcia Aristizabal et al. 2011, Hamdhan & Schweiger 2013, Mohd Taib et al. 2018). Zhang et al. (2004) added that apart from the intensity and duration of rainfall, the soil saturated permeability also influences the rate of infiltration. The Green-Ampt model is one of the common models used to observe and understand rainfall infiltration. Aside from the infiltration process alone, the soil-water characteristic curve and permeability determine the rate of infiltration also.

Since the partially saturated soil is formed above the phreatic level in regards to the cyclic drying and abundant rainfall, the SWCC and permeability functions are used to describe the water extraction and water infiltration during the rainfall period. This infiltration is highly influenced by water seepage in the soils. The SWCC as proposed by Fredlund et al. (1994) consists of the water content at specific suction, θ_w , and at saturation, θ_s , degree of saturation, S , suction given as the difference of pore-air pressure and pore-water pressure, $(u_a - u_w)$, e as a natural number, $C(\psi)$ as the correction factor and the three shape-parameters; a , n and m that refers to the air-entry value (AEV), pore size distribution and the slope of the SWCC respectively. The SWCC is given as:

$$\theta_w = C(\psi) \frac{\theta_s}{\{\ln[e + (u_a - u_w)/a]^n\}^m} \quad (1)$$

They further suggested an additional parameter which is the residual water content, θ_r as it will plot a sigmoidal curve. Leong et al. (1997i) also concluded that sigmoidal curve is more versatile and perform a better fit of the SWCC. Fredlund et al. (1994) discovered that when $C(\psi)$ is taken as 1.0, the equation can be used with less complexity. Therefore, the equation is given as Equation (2) and it is used in this study.

$$\theta_w = \theta_r \frac{\theta_s - \theta_r}{\{\ln[e + (\psi/a)^n]\}^m} \quad (2)$$

Furthermore, the permeability equation defines the coefficient of permeability with respect to water, k_w as a function of both the void ratio and water content (Leong et al. 1997ii). By using k_w which can be derived from the SWCC corresponding at any value of the water content, Childs et al. (1950) suggested the transformation of the SWCC with $\theta_w(\psi)$ into $\theta_w(r)$ where r is the pore radius. The transformation requires tedious work, thus, Marshall (1958) improved the permeability function and recommended the application of identical water content intervals leading to the following equation:

$$k_w(\theta_w) = \frac{T_s^2}{2\rho_w g \mu} \frac{n^2}{m^2} \sum_{i=1}^l \frac{2(i-1)-1}{\psi_i^2} \quad (3)$$

Where T_s is the surface tension of water, ρ_w is the density of water, μ the dynamic viscosity of water, n the porosity of soil, m as the total number of intervals given by $= (\theta_s/\Delta\theta_w)$, l as the number of intervals corresponding to θ_w given by $= (\theta_w/\Delta\theta_w)$, ψ_i as the matric suction corresponding to the midpoint of the i th interval of the SWCC. This permeability function has been adopted to calculate the saturated coefficient of permeability.

The saturated coefficient of permeability, k_{sat} , is one of the principal parameters of a permeability function. The saturated state, which represents the initial condition of a permeability function, determines the rates of water flow, specifically infiltration. The literature reveals that sensitivity analysis conducted with respect to the permeability function is undertaken by using different k_{sat} values. Tsaparas et al. (2002), Tsiampousi et al. (2013), Garcia Aristizabal et al. (2011), Zhang et al. (2004) and Rahimi et al. (2010) all studied the effects of permeability on slope behaviour. Generally, the saturated values were varied by an increment of 1E-1 m/s representing a range of high and low conductivity soils. Tsaparas et al. (2002) added that very permeable soils can be discovered at $k_{sat} = 1E-4$ m/s, moderately permeable at $k_{sat} = 1E-5$ to $1E-6$ m/s and low permeability soils at $k_{sat} = 1E-7$ m/s.

2.2 Groundwater seepage

The groundwater flow analysis is performed with an initial phase of steady-state and a series of transient seepage phases in Plaxis. The groundwater flow is generally governed by the fundamental Darcy's law and the continuity equations. The flow equation can be written in three dimensions as in Equation (4) (Galavi 2010).

$$\underline{q} = \frac{k}{\rho_w g} (\nabla p_w + \rho_w \underline{g}) \quad (4)$$

The terms q , k , g and ρ_w are the specific discharge (fluid velocity), permeability tensor, acceleration vector due to the gravity and the density of water, respectively. The groundwater flow is the resultant of the pore-water pressure gradient presented as ∇p_w . Nevertheless, the term $\rho_w g$ will be used because the flow is no longer affected by the gradient of pore-water pressure in a vertical direction when hydrostatic conditions are assumed. In unsaturated soil mechanics, the coefficient of permeability, \underline{k} is associated to soil saturation by:

$$\underline{k} = k_{rel} \times \underline{k}^{sat} \quad (5)$$

k_{rel} is the ratio of permeability at a particular saturation of the permeability in saturated state, \underline{k}^{sat} .

3 HYDROLOGICAL AND SOIL PROPERTIES

In this study, the basic mechanical and hydrological properties are described in Table 1. The soils used were classified as undisturbed samples. Based on the existing soil profile that has been analysed, two layers of soils are assigned in the models which are silty sand and sandy silt. It can be seen that the silty sand has a high cohesion value due to the high variability of residual soils in Bukit Timah Granite. The percentage of clayey material is accepted for silty sand in Singaporean soils. On the other hand, the sandy silt presents a zero value indicating very sandy materials. These layers of soils are modelled based on the slope geometry shown in Figure 1. Full dimensions, flux boundary conditions and location of the groundwater table are also illustrated in Figure 1. Moreover, the soil hydrological properties are calibrated from the SWCC and permeability functions showed in Figure 2 and 3, respectively. The analysis is simulated by using flow calculation in transient mode. The initial negative pore-water pressure (suction) profiles are generated by applying rainfall with the intensity of $1E-7$ m/s for two months onto the unsaturated soils. The typical rainfall pattern is shown in Figure 4. The evaporation and runoff, however, are not considered in the analyses to focus on the rainfall infiltration. The numerical modelling in the paper is undertaken by using Plaxis based on a case study by Mohd Taib et al. (2019).

Table 1. Mechanical and hydrological properties of soils (Mohd Taib et al. 2019).

Description	Silty sand	Sandy silt
Mechanical properties		
Effective cohesion, c' (kPa)	9.0	0
Effective angle of friction, ϕ' ($^\circ$)	34	33
Total density, ρ_t (Mg/m ³)	2.03	1.88
Specific gravity, G_s	2.66	2.58
Void ratio, e	0.8	0.86
Hydrological properties		
Saturated coefficient of permeability, k_s (m/s)	6E-6	3.3E-5
Saturated volumetric water content, θ_s	0.6	0.5306
Fitting parameter, a (kPa)	1.1	7.0
Fitting parameter, n	0.55	5.0
Fitting parameter, m	1.33	0.7
Air-entry value, (AEV)	15.0	5.0
Residual volumetric water content, θ_r	0.15	0.15
Residual suction ψ_r (kPa)	6000	22.0

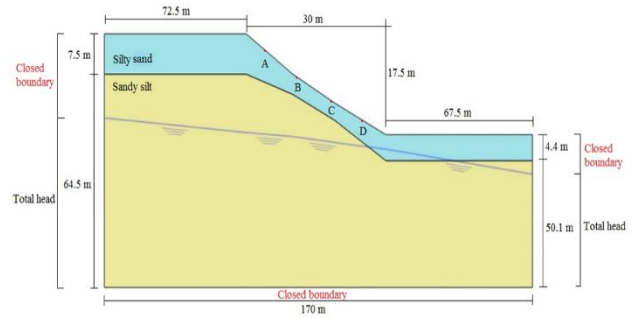


Figure 1. Slope geometry (Mohd Taib et al. 2019).

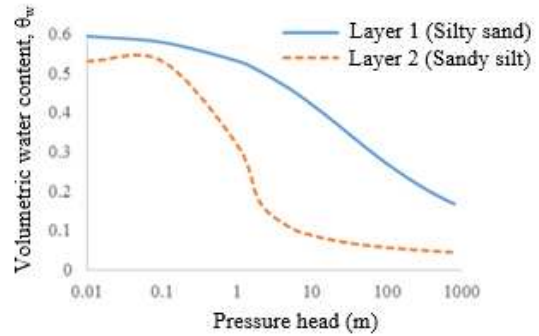


Figure 2. Soil-water characteristic curve (Mohd Taib et al. 2019).

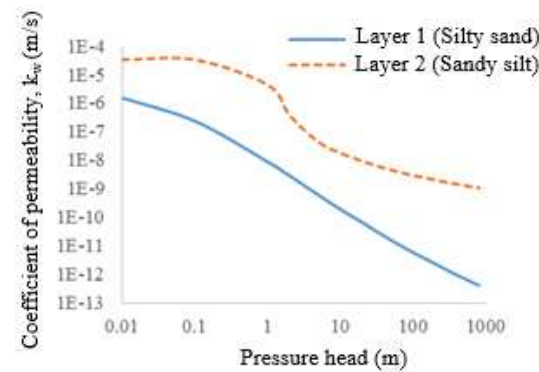


Figure 3. Permeability function (Mohd Taib et al. 2019).

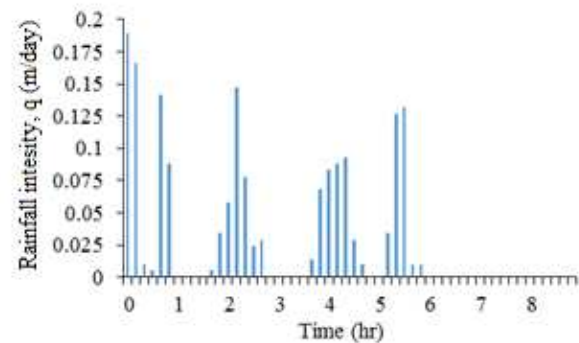


Figure 4. Typical rainfall intensity (Mohd Taib et al. 2019).

4 RESULTS AND DISCUSSION

The results of the studies are presented in two major categories of rainfall distribution which are the constant and cumulative intensities. The duration of rainfall (i.e. 9 hours) is kept constant based on the typical rainfall used. The analysis and discussion describe the two points of A and D as shown in Figure 1 representing the toe and the crest of the slope.

4.1 Constant rainfall

Figure 5 shows the pore-water pressure developed at the slope crest labelled as Location A. Constant rainfall was applied throughout the simulation periods for 9 hours. At a depth of 0.64 m where it is closest to the ground surface. There is an increase of pore-water pressure but the largest change is seen occurring at this location. By comparing to the toe of the slope marked as Location D, shown in Figure 6, the change of pore-water pressure is smaller. Ng et al. (2001) stated that the pore-water pressure on the ground surface increased immediately after the rainfall commenced. The high rate of pore-water pressure generated can be due to the fact that no ponding occurred considering the height and the slope angle. Rahimi et al. (2010) analysed their findings in the relationships between the safety factor and elapsed time. They noted that the safety factor decreased at the fastest rate for the advanced distribution of rainfall. It can be suggested here that the large change in pore-water pressure is also due to the constant rainfall applied, indicating rapid water infiltration.

In contrast, the lower depths at 1.31, 1.66 and 2.08 m indicated the slow rate of changes in the pore-water pressure generated. The pore-water pressure can be seen as a pattern that developed against time in the graphs. It is observed that the pattern was developed practically consistent during rainfall, but at a different range where the largest value was between -18 and -27 kPa at Location D and the smallest was between -27 and -31 kPa found at Location A. At the deepest measurement (i.e. 2.08m), the pore-water pressure was constant throughout the simulations which suggest that only minor changes of pore-water pressure can be captured at low depths. Ng et al. (2001) have proposed that the influence of rainfall patterns on pore-water pressure was most noticeable on the ground surface and that such effects gradually diminish with an increase in depth. The results in this section are broadly supported by the findings of Ng et al. (2001), where suction remained high at a lower depth compared to the ground surface.

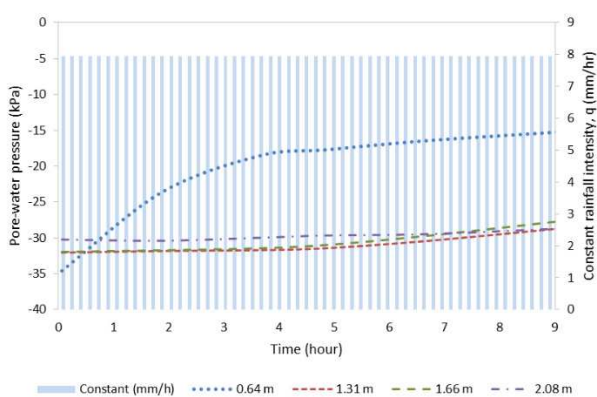


Figure 5. Constant rainfall using average typical rainfall intensity for location A.

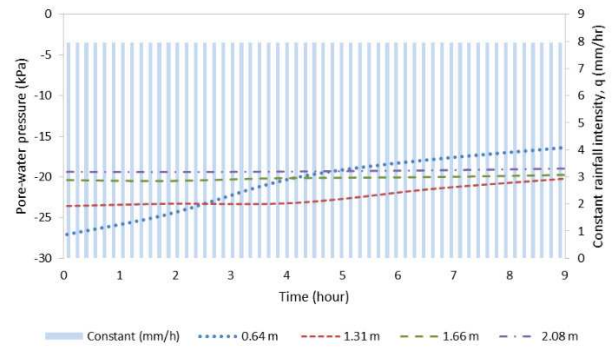


Figure 6. Constant rainfall using average typical rainfall intensity for location D.

4.2 Cumulative rainfall

Figure 7 illustrates the pore-water pressure generated as a result of cumulative rainfall at the same location of A and D. The trend of the pore-water pressure generated nearly followed the applied cumulative rainfall but at different rates. It is revealed that the pore-water pressure generated in the first hour at the nearest depth to the surface developed the highest negative pore-water pressure. The high pressure can be explained by the effects of drying on the ground surface, as a result of steady-state at the beginning of the simulations. As soon as rainfall is applied, the pore-water pressure increased, especially at shallower depths. The findings made by Ng et al. (2001) can be seen similarly in this situation, where the highest pore-water pressure was most visible at the surface when rainfall was applied. It also appeared for lower depths at 1.31, 1.66 and 2.08 m; the developed pore-water pressure was increasing according to depth. For all the patterns, it can be observed that the results calculated are very close from the 5th to the 7th hour. The cumulative rainfall is grouped into stages where there are three significant levels. Started from hour 5.5 onwards, the rainfall had accumulated at a high intensity of $1.08E-4$ m/s.

One possible explanation for this occurrence is that the rainfall is filling the voids and became more saturated. The gap where there is no increment of rainfall, allowed water to percolate into the soils and reduced the negative pore-water pressure. Similar to continuous rainfall analysis in previous Section 3.1, ponding and runoff are not considered in the simulations; hence, only loss of negative pore-water pressure is occurring. This scenario can be the reason why the rates of pore-water pressure generated at the toe and crest had changed. It can be seen that the pore-water pressure developed in the lowest depth (i.e. 2.08 m) changed rapidly at the toe. As the results were recorded for all depths, the pore-water pressure again increased. The trends are no longer smooth except for Location A. The pore-water pressure at this location revealed that saturation had been reached, while the rest of the locations were slowly developing the pore-water pressure with minimal fluctuations. This section proves that the pore-water pressure increases with cumulative rainfall intensity, not evenly but according to increasing depth.

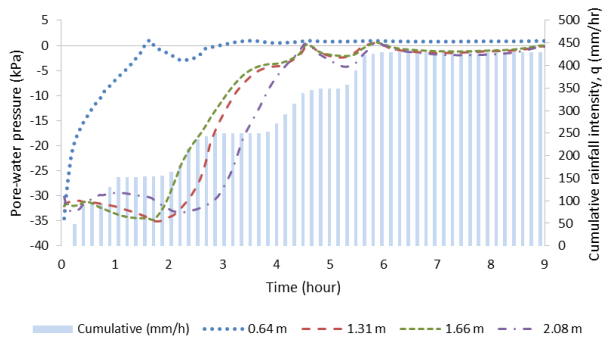


Figure 7. Cumulative rainfall using average typical rainfall intensity for location A.

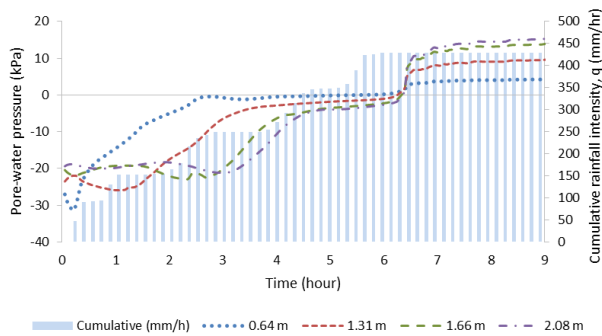


Figure 8. Cumulative rainfall using average typical rainfall intensity for location D.

5 CONCLUSIONS

The effects of rainfall patterns in modelling unsaturated groundwater flow were studied. Two major patterns namely the constant and cumulative rainfall were applied to represent the abundant rainfall during the wet season. By making the duration constant and the intensities varied, the changes of negative pore-water pressure particularly can be captured. For both occasions where constant and cumulative rainfall is applied, the slope crest shows the large changes of negative pore-water pressure compared to the toe. Moreover, the generation of negative pore-water pressure based on different depths shows that shallower depths are more susceptible to changes. This is due to the rapid water infiltration and the soils reaching saturation are at shallower depths faster than the deeper soils. It can be concluded that the intensity and different patterns of rainfall affect the initial pore-water pressure of unsaturated soils. In addition, other factors such as the slope height and angle, SWCC and soil permeability influences the rate of pore-water pressure changes in partially saturated soils as well.

6 ACKNOWLEDGEMENTS

The author would like to thank the people involved in the research project and acknowledge Universiti Kebangsaan Malaysia for financial support under the grant GUP-2021-022 and National Hydraulic Research Institute of Malaysia (NAHRIM) with grant KK-2020-009.

7 REFERENCES

Cai F. and Ugai K. 2004. Numerical Analysis of Rainfall Effects on Slope Stability. *International Journal of Geomechanics*, 4(2), 69-78.
 Che Ghani A.N., Mohd Taib A., and Abang Hasbollah D.Z. 2019. Effect of rainfall pattern on slope stability. in International Conference on

Geotechnics for Sustainable Infrastructure Development (GEOTEC HANOI).
 Childs E.C. and Collis-George N. 1950. The permeability of porous materials. *Proceedings of the Royal Society of London. Series A, Mathematical and Physical Sciences*, 201(1066), 392-405.
 El-Shafie A., Mazoghi H., AbouKheira A., and Taha M.R. 2011. Artificial neural network technique for rainfall forecasting applied to Alexandria, Egypt. *International Journal of the Physical Sciences*, 6, 1306-1316.
 Fredlund D.G. and Xing A. 1994i. Equations for the soil-water characteristic curve. *Canadian Geotechnical Journal*, 31(3), 521-532.
 Fredlund D.G., Xing A., and Huang S. 1994ii. Predicting the permeability function for unsaturated soils using the soil-water characteristic curve. *Canadian Geotechnical Journal*, 31(4), 533-546.
 Galavi V. 2010. Groundwater flow, fully coupled flow deformation and undrained analyses in PLAXIS 2D and 3D, Plaxis BV.
 Garcia Aristizabal E.F., Riveros Jerez C.A. and Builes Brand M.A. 2011. Influence of rainfall intensity on infiltration and deformation of unsaturated soil slopes. *DYNA*, 78, 116-124.
 Gasmo J.M., Rahardjo H. and Leong E.C. 2000. Infiltration effects on stability of a residual soil slope. *Computers and Geotechnics*, 26(2), 145-165.
 Gofar N., Lee L.M. and Kassim A. 2008. Response of suction distribution to rainfall infiltration in soil slope. *Electronic Journal of Geotechnical Engineering*, EJGE, 13, 1-13.
 Hamdhan I.N. and Schweiger H.F. 2013. Finite element method based analysis of an unsaturated soil slope subjected to rainfall infiltration. *International Journal of Geomechanics*.
 Ibrahim A., Ahmad I.K. and Taha M.R., 2018. 3 Dimension real time images of rainfall infiltration into unsaturated soil slope. *International Journal of GEOMATE*, 14(43), 31-35.
 Kristo C., Rahardjo H., and Satyanaga A. 2017. Effect of variations in rainfall intensity on slope stability in Singapore. *International Soil and Water Conservation Research*, 5(4), 258-264.
 Leong E.C. and Rahardjo H. 1997i. Review of soil-water characteristic curve equations. *Journal of geotechnical and geoenvironmental engineering*, 123(12), 1106-1117.
 Leong E.C. and Rahardjo H. 1997ii. Permeability functions for unsaturated soils. *Journal of Geotechnical and Geoenvironmental Engineering*, 123(12), 1118-1126.
 Li Z., Yongjun He, Hongen Li, and Yanqiao Wang. 2017. Antecedent rainfall induced shallow landslide-A case study of Yunnan landslide, China. 26.
 Marshall T.J. 1958. A relation between permeability and size distribution of pores. *Journal of Soil Science*, 9(1), 1-8.
 McDougall J.R. and Pyrah I.C. 1998. Simulating transient infiltration in unsaturated soils. *Canadian geotechnical journal*, 35(6), 1093-1100.
 Mohd Taib A. 2018. Numerical modelling of unsaturated tropical slopes, in School of Engineering, Newcastle University: Newcastle upon Tyne, UK.
 Mohd Taib A., Taha M.R. and Abang Hasbollah D.Z. 2018. Validation of Numerical Modelling Techniques in Unsaturated Slope Behaviour. *Jurnal Kejuruteraan*, 5(Special Issue 1), 29-35.
 Mohd Taib A., Taha M.R. and Abang Hasbollah D.Z. 2019. Influence of Initial Conditions on Unsaturated Groundwater Flow Models. *International Journal of Engineering & Technology*, 8(1.2), 34-40.
 Mukhlisin M., Baidillah M.R., Taha M.R. and El-Shafie A. 2011. Effect of soil water retention model on slope stability analysis. *International Journal of Physical Sciences*, 6(19), 4629-4635.
 Ng C.W., Wang B. and Tung Y.K. 2001. Three-dimensional numerical investigations of groundwater responses in an unsaturated slope subjected to various rainfall patterns. *Canadian Geotechnical Journal*, 38(5), 1049-1062.
 Ng C.W.W. and Shi Q. 1998. Influence of rainfall intensity and duration on slope stability in unsaturated soils. *Quarterly Journal of Engineering Geology and Hydrogeology*, 31(2), 105-113.
 Rahardjo H., Li X.W., Toll D.G. and Leong E.C. 2001. The effect of antecedent rainfall on slope stability, in *Unsaturated Soil Concepts and Their Application in Geotechnical Practice*, Springer. 371-399.
 Rahimi A., Rahardjo H. and Leong E.C. 2010. Effect of antecedent rainfall patterns on rainfall-induced slope failure. *Journal of Geotechnical and Geoenvironmental Engineering*, 137(5), 483-491.
 Sagitaningrum F. and Bahsan E. 2017. Parametric study on the effect of rainfall pattern to slope stability. *MATEC Web of Conferences*, 101, 05005.

- Taha M.R., Hossain M.K. and Mofiz S.A., 2000. Effect of suction on the strength of unsaturated soil. In *Advances in Unsaturated Geotechnics*, 210-221.
- Toll D.G. 2001. Rainfall-induced landslides in Singapore. *Geotechnical Engineering*, 149(4), 211-216.
- Tsaparas I., Rahardjo H., Toll D.G. and Leong E.C. 2002. Controlling parameters for rainfall-induced landslides. *Computers and Geotechnics*, 29(1), 1-27.
- Tsiampousi A., Zdravković L. and Potts D.M. 2013. Variation with time of the factor of safety of slopes excavated in unsaturated soils. *Computers and Geotechnics*, 48(0), 167-178.
- Van Genuchten M.T. 1980. A closed-form equation for predicting the hydraulic conductivity of unsaturated soils. *Soil Science Society of America Journal*, 44(5), 892-898.
- Zhan T.L.T. and Ng C.W.W. 2004. Analytical analysis of rainfall infiltration mechanism in unsaturated soils. *International Journal of Geomechanics*, 4(4), 273-284.
- Zhan T.L.T., Ng C.W.W. and Fredlund D.G. 2007. Field study of rainfall infiltration into a grassed unsaturated expansive soil slope. *Canadian Geotechnical Journal*, 44(4), 392-408.
- Zhang L.L., Fredlund D.G., Zhang L.M. and Tang W.H. 2004. Numerical study of soil conditions under which matric suction can be maintained. *Canadian Geotechnical Journal*, 41(4), 569-582.